Design of Acoustic Vehicle Detector with Steady-Noise Suppression

Shigemi Ishida[1], Masato Uchino[1], Chengyu Li[1], Shigeaki Tagashira[2], and Akira Fukuda[1]

***Abstract*— Vehicle detection is a basic component for many applications in intelligent transportation system (ITS). We are developing a low-cost vehicle detector relying on sound arrival time difference on two microphones. Our previous paper presented that our acoustic vehicle detector successfully detected vehicles with an F-measure of 83 %. However, the acoustic detector has difficulties in vehicle detection in an environment with steady noise such as rain noise.**

This paper presents a steady-noise suppression method for the acoustic vehicle detector. Our key idea is to exclude the influence of steady noise in a sound delay estimation. The acoustic vehicle detector estimates vehicle sound delay by finding a peak on a cross-correlation function. We theoretically analyze the influence of steady noise and remove a peak caused by the noise to minimize the influence. Experimental evaluations revealed that the steady-noise suppression method effectively reduced the noise influence and resulted in F-measures of 0.92 and 0.90 in normal and heavy rain conditions, respectively.

I. Introduction

Recent development of computing and sensing technologies has led to many new intelligent transportation system (ITS) applications. ITS applications are mainly designed to improve safety, efficiency, accessibility, and dependability of transportation. A car navigation system considering traffic jam, automatic cruising system, and self-driving car are typical examples of ITS.

Vehicle detection is a basic component for many applications in ITS. Typical examples of vehicle sensors are loop coils, photoelectric tubes, laser, and ultrasound sensors, which are installed on or above roads. These vehicle sensors, however, require roadwork closing target road sections for deployment and maintenance. In Japan, vehicle sensors are only available on high traffic roads and highways because of the deployment and maintenance costs. There are CCTV-based and probe car-based low-cost vehicle detectors [1–9], which are applicable to high traffic roads.

We also have presented a low-cost vehicle detector relying on stereo microphones installed at a sidewalk [10]. Our acoustic vehicle detector estimates vehicle sound arrival time difference, i.e., sound delay, between two microphones to detect vehicles. We experimentally demonstrated that the acoustic vehicle detector successfully detected vehicles with an F-measure of 83 %.

This work was supported in part by JSPS KAKENHI Grant Numbers JP15H05708, JP17H01741, and JP18K18041.

[1]S. Ishida, C Li, M Uchino, and A. Fukuda are with the Graduate School and Faculty of Information Science and Electrical Engineering, Kyushu University, Fukuoka 819-0395, Japan (email: {ishida, uchino, licy0012, fukuda}@f.ait.kyushu-u.ac.jp)

[2]S. Tagashira is with the Faculty of Informatics, Kansai University, Osaka 569-1095, Japan (email: shige@res.kutc.kansai-u.ac.jp)

The acoustic vehicle detector, however, has difficulties in vehicle detection in a noisy environment, especially in an environment with steady noise such as a rain sound. The acoustic vehicle detector estimates vehicle sound delay by finding a peak on a cross-correlation of sound signals received on two microphones. The steady noise generates a peak and weaken the peak caused by a vehicle sound.

To tackle the steady noise problem, we present a steady-noise suppression method for the acoustic vehicle detector. Our key idea is to mathematically exclude the influence of steady noise in a sound delay estimation. We formulate the noise influence in a sound delay estimation and remove a peak using steady-noise data prior to peak detection. The steady-noise data is updated when no vehicle is passing because noise signals are actually quasi-steady and are changing in a long time. The experimental evaluations revealed that the proposed steady-noise suppression method successfully improved vehicle detection accuracy by 4 and 13 % in normal and heavy rain conditions, respectively.

Specifically, our key contributions are threefold:

- We theoretically analyze the influence of steady noise in an acoustic vehicle detector.
- We present a steady-noise suppression method based on the theoretical analysis. To the best of knowledge, this is a first trial to reduce the influence of noise in acoustic vehicle sensing.
- We experimentally compare the performance of vehicle detector between with and without the steady-noise suppression.

The remainder of this paper is organized as follows. Section II briefly describes an acoustic vehicle detector presented in our previous paper and analyzes the influence of noise. We design a steady-noise suppression method in Section III and Section IV presents experimental evaluations to demonstrate the effectiveness of the noise suppression method. Section V looks through related works on acoustic noise reduction methods. Finally, Section VI concludes the paper.

II. Acoustic Vehicle Detector

A. Overview of Vehicle Detector

Figure 1 shows an overview of an acoustic vehicle detector presented in our previous paper [10], which consists of a sound retriever, sound mapper, and vehicle detector. A sound retriever is stereo microphones followed by low-pass filters (LPFs). We install stereo microphones at a sidewalk and apply a LPF with a cut-off frequency of 2.5 kHz to the sound signals because majority of frequency components of vehicle

This is an accepted version of the paper.

doi: 10.1109/ITSC.2019.8917289

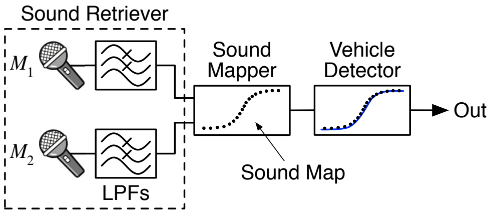

Fig. 1. Overview of acoustic vehicle detector [10]

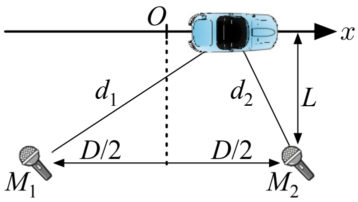

Fig. 2. Microphone setup [10]

sound are less than 2.0 kHz [11]. A sound mapper estimates vehicle sound delay, i.e., time difference of sound arrival, on the two microphones and draws a *sound map*, which is a map of the sound delay as a function of time. A vehicle detector finally analyzes the sound map to detect vehicles.

As shown in Fig. 2, two microphones M_1 and M_2 separated by distance D are installed at a sidewalk L away from the road center. Let x be the location of a vehicle. When a vehicle is passing $x = 0$ at time $t = 0$ at a constant speed of v, sound delay Δt is calculated by the difference of distance d_1 and d_2 as:

$$\begin{aligned}\Delta t &= \frac{d_1 - d_2}{c} \\ &= \frac{1}{c}\left\{\sqrt{\left(vt + \frac{D}{2}\right)^2 + L^2} - \sqrt{\left(vt - \frac{D}{2}\right)^2 + L^2}\right\},\end{aligned} \tag{1}$$

where c is the speed of sound in air. Equation (1) indicates that a passing vehicle draws an S-curve. Figure 3 shows an example of sound map. Two S-curves indicate that two vehicles were passing. The S-curves are detected using

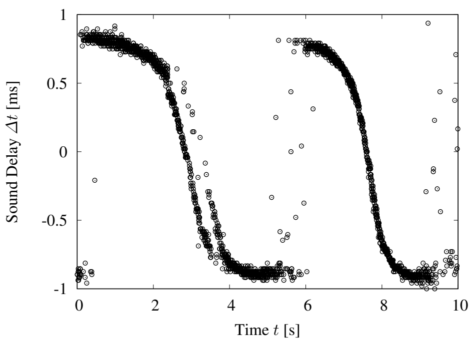

Fig. 3. Sound map example

a random sample consensus (RANSAC) robust estimation algorithm [12].

B. Sound Delay Estimation in Noisy Environment

We first formulate a sound delay estimation in a noise-free environment. The sound mapper estimates a sound delay using a cross-correlation function. We use generalized cross-correlation phase transform (GCC-PHAT) instead of normal cross-correlation. Let $s_1(t)$ and $s_2(t)$ be sound signals on two microphones, $S_1(f)$ and $S_2(f)$ be frequency-domain representation of $s_1(t)$ and $s_2(t)$, respectively. GCC $R^P_{s_1 s_2}(t)$ between sound signals $s_1(t)$ and $s_2(t)$ is defined as:

$$R^P_{s_1 s_2}(t) = \int \frac{G_{s_1 s_2}(f)}{|G_{s_1 s_2}(f)|} e^{j2\pi f t}\, df, \tag{2}$$

where

$$G_{s_1 s_2}(f) = \overline{S_1(f)} S_2(f). \tag{3}$$

Assume that we receive the same sound signals with sound delay Δt on the two microphones, i.e., $s_2(t) = \alpha s_1(t - \Delta t)$, where α is an amplitude scaling factor. We can rewrite Eq. (3) as:

$$G_{s_1 s_2}(f) = \alpha e^{-j2\pi f \Delta t} |S_1(f)|^2. \tag{4}$$

GCC is therefore calculated to be:

$$\begin{aligned}R^P_{s_1 s_2}(t) &= \int e^{j2\pi f (t - \Delta t)}\, df \\ &= \delta(t - \Delta t),\end{aligned} \tag{5}$$

where $\delta(\tau)$ is a delta function. We can estimate Δt by finding a peak of GCC.

In a noisy environment, sound signals are mixtures of vehicle sound $v_1(t)$, $v_2(t)$ and noise $n_1(t)$, $n_2(t)$ signals. Sound signals received on the two microphones in a noisy environment are described as:

$$s_1(t) = v_1(t) + n_1(t), \tag{6a}$$

$$s_2(t) = v_2(t) + n_2(t) = \alpha v_1(t - \Delta t) + n_2(t). \tag{6b}$$

We derive GCC:

$$R^P_{s_1 s_2}(t) = V(t) \otimes \delta(t - \Delta t) + N(t), \tag{7}$$

where $\otimes$ represents a convolution operation and

$$V(t) = \int \frac{\alpha G_{v_1 v_1}(f)}{|\alpha G_{v_1 v_1}(f) e^{-j2\pi f \Delta t} + G_{n_1 n_2}(f)|} e^{j2\pi f t}\, df, \tag{8a}$$

$$N(t) = \int \frac{G_{n_1 n_2}(f)}{|\alpha G_{v_1 v_1}(f) e^{-j2\pi f \Delta t} + G_{n_1 n_2}(f)|} e^{j2\pi f t}\, df. \tag{8b}$$

Figure 4 shows examples of GCC $R^P_{s_1 s_2}(t)$ calculated over sound signals derived in no-rain and raining conditions. Although the GCC in no rain conditions gives a clear peak, many sub-peaks appear in the GCC in raining condition, which makes it difficult to find a peak corresponding to a vehicle. Figure 5 shows a sound map example in raining conditions, which suffers from many noise points caused by an incorrect sound-delay estimation.

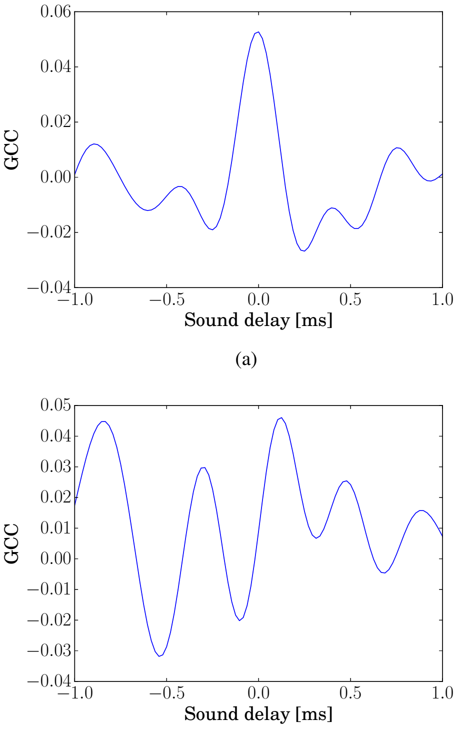

(b)

Fig. 4. Example of GCC in (a) no rain and (b) raining conditions

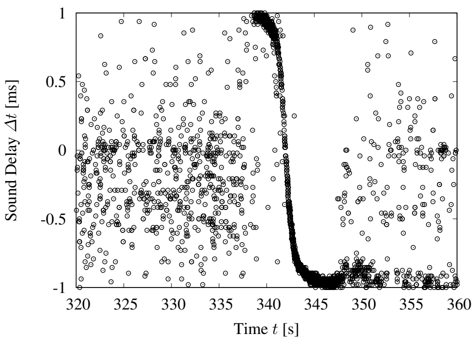

Fig. 5. Sound map example under raining condition

III. Steady-Noise Suppression

A. Key idea

The key idea of steady-noise suppression is to move GCC noise peaks to a specific sound delay value. The location of GCC noise peaks randomly changes time to time. We perform a specific signal processing to move GCC noise peaks at a constant sound delay that is physically impossible as a vehicle delay.

Figure 6 shows an overview of a sound retriever block with steady-noise suppression. Compared to a sound retriever in Fig. 1, we add couple of blocks to add specific signals calculated from noise data stored in a *noise storage* block. The

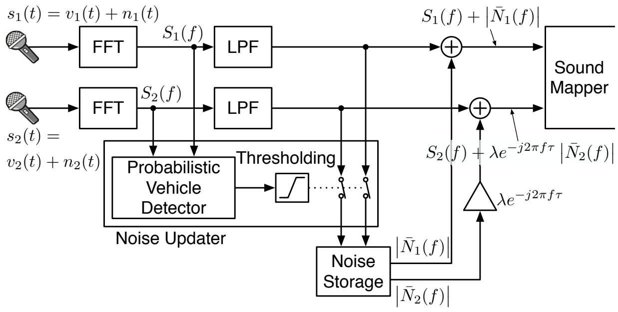

Fig. 6. Overview of sound retriever block with steady-noise suppression

noise storage block holds frequency component information of steady-noise signals, which is updated when no vehicle is passing. The following subsections give design details of a noise suppression method.

B. Sound Delay Estimation with Steady-Noise Suppression

Let $\bar{N}_1(f)$ and $\bar{N}_2(f)$ be frequency-domain representation of steady-noise signals on two microphones. As shown in Fig. 6, a sound mapper receives sound signals $\bar{S}_1(f)$ and $\bar{S}_2(f)$ given by equations below:

$$\bar{S}_1(f) = V_1(f) + N_1(f) + \left|\bar{N}_1(f)\right|, \tag{9a}$$

$$\bar{S}_2(f) = V_2(f) + N_2(f) + \lambda e^{-j2\pi f\tau} \left|\bar{N}_2(f)\right|, \tag{9b}$$

where λ (≥ 1) is a positive real constant number named *noise supplement factor* and τ is a real constant number named *noise delay*. When a vehicle sound and noise signals are uncorrelated, GCC $R^P_{\bar{s}_1\bar{s}_2}(t)$ is calculated to be:

$$R^P_{\bar{s}_1\bar{s}_2}(t) = R^P_{v_1v_2}(t) + R^P_{n_1n_2}(t) + \lambda R^P_{\bar{n}_1\bar{n}_2}(t), \tag{10}$$

where $R^P_{v_1v_2}(t)$, $R^P_{n_1n_2}(t)$, and $R^P_{\bar{n}_1\bar{n}_2}(t)$ are GCCs of a vehicle sound, noise, and stored noise, respectively, which are given by:

$$R^P_{v_1v_2}(t) = \int \frac{G_{v_1v_2}(f)}{|G_{\bar{s}_1\bar{s}_2}(f)|} e^{j2\pi ft}\, df, \tag{11a}$$

$$R^P_{n_1n_2}(t) = \int \frac{G_{n_1n_2}(f)}{|G_{\bar{s}_1\bar{s}_2}(f)|} e^{j2\pi ft}\, df, \tag{11b}$$

$$R^P_{\bar{n}_1\bar{n}_2}(t) = \int \frac{G_{|\bar{n}_1||\bar{n}_2|}(f)}{|G_{\bar{s}_1\bar{s}_2}(f)|} e^{j2\pi f(t-\tau)}\, df. \tag{11c}$$

When noise signals are very similar to the stored noise, i.e., $N_1(f) \approx \bar{N}_1(f)$ and $N_2(f) \approx \bar{N}_2(f)$,

$$\left[R^P_{|\bar{n}_1||\bar{n}_2|}(t)\right]_{\text{MAX}} > \left[R^P_{n_1n_2}(t)\right]_{\text{MAX}}. \tag{12}$$

Equation (12) implies that GCC $R^P_{\bar{s}_1\bar{s}_2}(t)$ tends to be dominated by stored noise signals $\bar{N}_1(f)$ and $\bar{N}_2(f)$ when no vehicle is passing and $\lambda \geq 1$. We can control the location of a GCC peak corresponding to $R^P_{\bar{s}_1\bar{s}_2}(t)$ by changing a noise delay τ because the peak of $R^P_{\bar{s}_1\bar{s}_2}(t)$ appears at $t = \tau$. Maximum vehicle-sound delay is restricted by a physical setup of microphones. We can easily remove sound map points corresponding GCC peaks caused by noise signals

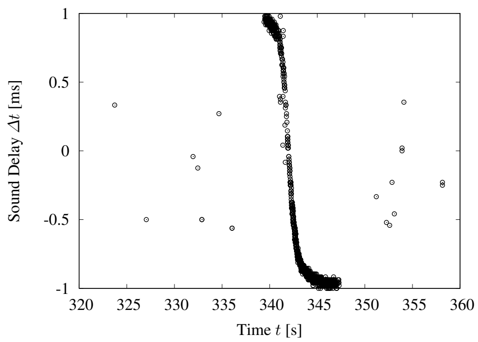

Fig. 7. Sound map example with noise suppressor

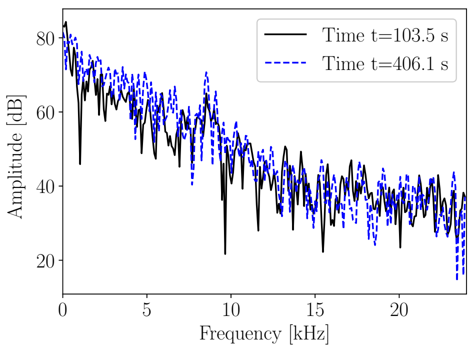

Fig. 8. Examples of rain noise frequency components at time $t = 103.45$ s and 406.15 s. Time difference is $406.1 - 103.5 = 302.6$ s ($\simeq 5$ minutes).

by choosing a noise delay τ to be an impossible delay for vehicles.

When a vehicle is passing, we can assume that GCC of vehicle sound signals is bigger than that of stored noise signals:

$$\left[R^P_{v_1 v_2}(t)\right]_{\mathrm{MAX}} > \left[R^P_{|\bar{n}_1||\bar{n}_2|}(t)\right]_{\mathrm{MAX}}. \tag{13}$$

In this case, a GCC peak is likely to correspond to a vehicle sound delay Δt.

When a noise supplement factor λ is too large, a GCC component $\lambda R^P_{\bar{n}_1 \bar{n}_2}(t)$ of stored noise signals in Eq. (10) cannot be ignored. We experimentally adjust λ based on the magnitude of a vehicle sound and noise signals.

Figure 7 shows an example of sound map with noise suppression. We set $\lambda = 1$ and $\tau = 4$ milliseconds in this figure. Compared to the original sound map shown in Fig. 5, we can confirm that the noise suppression successfully reduces sound map points that seem to be caused by a rain noise. An S-curve clearly appears on a sound map, which is easily detected by a RANSAC algorithm.

C. Noise data update

Because we are assuming that noise signals are very similar to a stored noise in Eq. (12), stored noise data needs to be updated to follow the change of quasi-steady noise

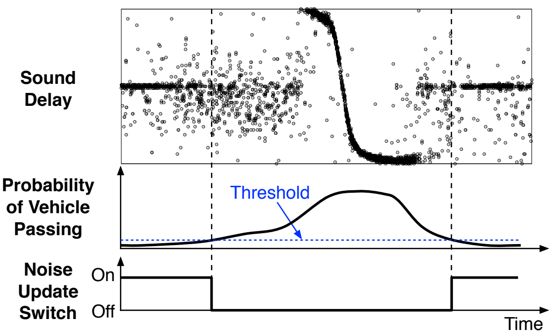

Fig. 9. Example of noise update process

signals in a long time. Figure 8 shows an example of the change in rain-noise frequency components in approximately five minutes. Even for a rain noise, frequency components changed in a long time, such as at 1 kHz, from 5 to 10 kHz, and at 23 kHz, as shown in Fig. 8.

Stored noise data is regularly updated by a noise updater, as shown in Fig. 6. The noise updater consists of probabilistic vehicle detector and thresholding blocks. The probabilistic vehicle detector calculates probability of vehicle passing. We apply thresholding to the probability to control input switches of a noise storage to update noise data stored in the noise storage when no vehicle is passing.

Figure 9 shows an example of a noise update process. Switches to a noise storage are only turned on when the probability of vehicle passing is lower than a threshold. We use a very low threshold to surely store noise data. When a vehicle is passing and the probability of vehicle-passing goes higher than the threshold, we stop the noise update to avoid storing a vehicle sound as a noise.

We can use any probabilistic vehicle detector for the noise update as long as the detector calculates probability of vehicle passing. Although we do not put a limit on the probabilistic vehicle detector, we employ an ultra low-power vehicle detection method presented in [13] in our evaluation.

IV. Evaluation

To demonstrate the effectiveness of our steady-noise suppression method, we conducted experimental evaluations on a road in our university campus.

A. Experiment Setup

Figure 10 shows an experiment setup. A target road in our university campus has two lanes, one lane in each direction. Two microphones, separated by $D = 30$ centimeters, were installed approximately $L = 2$ meters away from the road center on a tripod at a height of approximately 1 meter. Maximum sound delay is calculated to be $D/c \simeq 0.88$ milliseconds in this setup. We recorded a vehicle sound using a Sony HDR-MV1 recorder with AZDEN SGM-990 microphones. The sound was recorded at a sampling rate of 48 kHz and with code length of 16 bits. We also recorded a video monitoring the road as ground truth data.

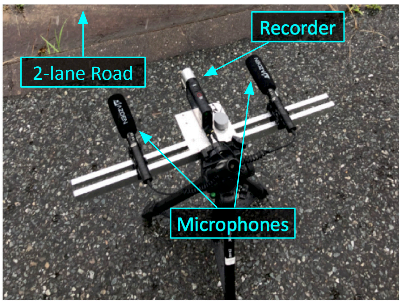

Fig. 10. Experiment setup

Vehicle sound was collected in normal and heavy rain conditions. We collected a vehicle sound for approximately 23 and 45 minutes, for which 93 and 165 vehicles passed, in normal and heavy rain conditions, respectively.

Using the collected sound data, we performed vehicle detection presented in [10] with the sound retriever presented in Section III. A noise supplement factor and noise delay were set to $\lambda = 1$ and $\tau = 4$ milliseconds, respectively.

We calculated an F-measure to evaluate vehicle detection performance, which is a commonly used metric in classification/detection problems. We first counted the numbers of true positives (TPs), false negatives (FNs), and false positives (FPs). We then calculated F-measure defined as:

$$\mathrm{Precision} = \frac{\mathrm{TP}}{\mathrm{TP} + \mathrm{FP}}, \tag{14a}$$

$$\mathrm{Recall} = \frac{\mathrm{TP}}{\mathrm{TP} + \mathrm{FN}}, \tag{14b}$$

$$\mathrm{F}_{\mathrm{measure}} = \frac{2 \cdot \mathrm{Precision} \cdot \mathrm{Recall}}{\mathrm{Precision} + \mathrm{Recall}}. \tag{14c}$$

TPs, FNs, and FPs are defined as the cases that a vehicle is detected when a vehicle is passing, that no vehicle is detected when a vehicle is passing, and that a vehicle is detected when no vehicle is passing, respectively.

B. *Vehicle Detection Performance*

Table I shows vehicle detection performance in (a) normal and (b) heavy rain conditions. Table I indicates the following:

- An F-measure of the vehicle detection system with the steady-noise suppression in normal rain conditions was 0.92. Compared to the vehicle detection without the noise suppression, an F-measure was increased by 4 %. In heavy rain conditions, an F-measure with the noise suppression was 0.90, which is 14 % higher than that without the noise suppression. In heavy rain conditions, the noise suppression effectively reduced the influence of a rain noise.
- A recall was significantly improved by our steady-noise suppression method. The steady-noise suppression method reduced sound map points caused by a rain noise, which greatly decreased the number of FN detections, resulting in 7 % and 20 % improvement in normal and heavy rain conditions, respectively.

TABLE I

VEHICLE DETECTION PERFORMANCE

(a) in normal rain conditions

	w/ Noise Suppression			w/o Noise Suppression		
	Left to Right	Right to Left	Total	Left to Right	Right to Left	Total
TPs	39	41	80	34	39	73
FNs	12	1	13	17	3	20
FPs	0	1	1	0	0	0
Precision	1.00	0.98	0.99	1.00	1.00	1.00
Recall	0.77	0.98	0.86	0.67	0.93	0.79
F-measure	0.87	0.98	0.92	0.80	0.96	0.88

(b) in heavy rain conditions

	w/ Noise Suppression			w/o Noise Suppression		
	Left to Right	Right to Left	Total	Left to Right	Right to Left	Total
TPs	74	62	136	54	49	103
FNs	20	9	29	40	22	62
FPs	0	0	0	0	0	0
Precision	1.00	1.00	1.00	1.00	1.00	1.00
Recall	0.79	0.87	0.82	0.57	0.69	0.62
F-measure	0.88	0.93	0.90	0.73	0.82	0.76

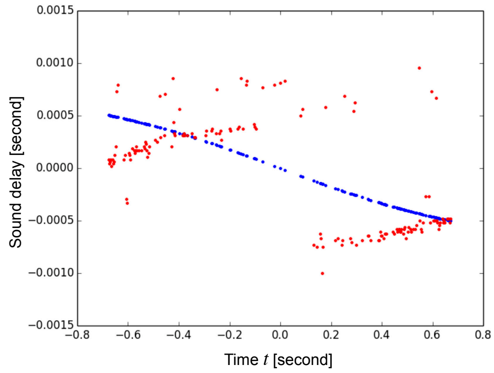

Fig. 11. Sound map with FP detection. Red and blue points represent sound map points and an estimated S-curve, respectively.

- Precision were nearly 100 % both in normal and heavy rain conditions. An acoustic vehicle detector itself is robust to a noise in terms of FP detections because the detector relies on S-curves drawn on sound map to detect vehicles. Only clear S-curves were detected by a RANSAC algorithm.
- Comparing Tables Ia and Ib, we can confirm that an F-measure in heavy rain conditions decreased by 12 points compared to that in normal rain conditions without the noise suppression. Heavy rain drastically degraded the vehicle detection performance. On the other hand, the decrease in an F-measure was 2 points with the noise suppression.

The above results confirm that our steady-noise suppression method effectively reduced the influence of a rain noise and increased an F-measure by up to 14 %, achieving an F-measure of up to 0.92.

In normal rain conditions, a FN detection occurred with the steady-noise suppression, as shown in Table I. Figure 11 shows a sound map with the FP detection. Red and blue points in Fig. 11 represent sound map points and an S-curve estimated from the sound map points, respectively. The FP was caused by sequentially passing vehicles, which is one of the known issues in our acoustic vehicle detector. Without the noise suppression, two sequential vehicles were not detected and became two FNs in Fig. 11, resulted in no FP detection. On the other hand, the steady-noise suppressor unveiled the sequential vehicle problem as two S-curves became sufficiently clear to be detected.

V. Related Works

To the best of knowledge, this paper is a first attempt to reduce the influence from steady-noise in an acoustic vehicle detector. In this section, we briefly look through acoustic noise reduction methods.

For noise reduction, empirical mode decomposition (EMD) based approaches have been reported [14–16]. Sound signals are decomposed into frequency components using EMD, which are more divided into signals and noises based on an intrinsic mode function (IMF) of the each frequency component. The EMD-based methods find a noise based on the characteristics of a noise. The characteristics of a noise, however, are dependent on a noise source, which makes difficult to apply to the acoustic vehicle detector because we cannot restrict a noise source in our scenario. Moreover, the EMD-based methods require at least three microphones at a specific configuration increasing deployment costs, while we are using two microphones with small constraints.

A noise reduction method steered response power phase transform (SRP-PHAT) using a microphone array has also been proposed [17]. This method reduces noise by combining SRP and GCC, both of which are used as sound source localization methods. SRP-PHAT subtracts noise power calculated from GCC over time-shifted sound signals to improve source localization accuracy. In our case, the average of GCC over noise signals is almost zero for steady noise. SRP-PHAT has small effect on steady-noise reduction.

For environmental noise reduction, soft thresholding (STH) based approach has been proposed [18]. This method decomposes sound signals by Wavelet transform and applies a soft threshold to distinguish noise components from a target sound. Although the STH-based approach is effective in environmental noise reduction, time-frequency characteristics of noise and sound must be different. We again cannot restrict a noise source in our scenario.

VI. Conclusion

In this paper, we presented a steady-noise suppression method for an acoustic vehicle detector to reduce the influence of a steady noise. Our key idea is to remove the influence of a noise in a sound delay estimation. The acoustic vehicle detector estimates vehicle sound delay on two microphones by finding a peak on a cross-correlation function. We perform a specific signal processing to move peaks on a cross-correlation caused by noise signals, avoiding incorrect peak detection. Experimental evaluations revealed that our steady-noise suppression method effectively reduced the influence of a noise and achieved vehicle detection with F-measures of 0.92 and 0.90 in normal and heavy rain conditions, respectively.

References

[1] N. Buch, M. Cracknell, J. Orwell *et al.*, "Vehicle localisation and classification in urban CCTV streams," in *Proc. ITS World Congress*, Sep. 2009, pp. 1–8.

[2] A. Nurhadiyatna, B. Hardjono, A. Wibisono *et al.*, "ITS information source: Vehicle speed measurement using camera as sensor," in *Proc. Int. Conf. on Advanced Computer Science and Information Systems (ICACSIS)*, Dec. 2012, pp. 179–184.

[3] C. de Fabritiis, R. Ragona, and G. Valenti, "Traffic estimation and prediction based on real time floating car data," in *Proc. IEEE Conf. Intelligent Transportation Systems (ITSC)*, Oct. 2008, pp. 197–203.

[4] D. B. Work, O.-P. Tossavainen, S. Blandin *et al.*, "An ensemble Kalman filtering approach to highway traffic estimation using GPS enabled mobile devices," in *Proc. IEEE Decision and Control (CDC)*, Dec. 2008, pp. 5062–5068.

[5] F. Calabrese, M. Colonna, P. Lovisolo *et al.*, "Real-time urban monitoring using cell phones – a case study in Rome," *IEEE Trans. Intell. Transp. Syst.*, vol. 12, no. 1, pp. 141–151, Mar. 2011.

[6] X. Zhou, W. Wang, and L. Yu, "Traffic flow analysis and prediction based on GPS data of floating cars," in *LNEE*, vol. 210, Nov. 2012, pp. 497–508, proc. Int. Conf. on Information Technology and Software Engineering.

[7] G. Guido, V. Galleli, F. Saccomanno *et al.*, "Treating uncertainty in the estimation of speed from smartphone traffic probes," *Transporation Research Part C: Emerging Technologies*, vol. 47, pp. 100–112, Oct. 2014.

[8] T. Seo, T. Kusakabe, and Y. Asakura, "Estimation of flow and density using probe vehicles with spacing measurement equipment," *Transporation Research Part C: Emerging Technologies*, vol. 53, pp. 134–150, Apr. 2015.

[9] T. Seo and T. Kusakabe, "Probe vehicle-based traffic state estimation method with spacing information and conservation law," *Transporation Research Part C: Emerging Technologies*, vol. 59, pp. 391–403, Oct. 2015.

[10] S. Ishida, J. Kajimura, M. Uchino *et al.*, "SAVeD: Acoustic vehicle detector with speed estimation capable of sequential vehicle detection," in *Proc. IEEE Conf. Intelligent Transportation Systems (ITSC)*, Nov. 2018, pp. 906–912.

[11] H. Wu, M. Siegel, and P. Khosla, "Vehicle sound signature recognition by frequency vector principal component analysis," in *Proc. IEEE Instrumentation and Measurement Technology Conf. (IMTC)*, vol. 1, May 1998, pp. 429–434.

[12] M. A. Fischler and R. C. Bolles, "Random sample censensus: A paradigm for model fitting with applications to image analysis and automated cartography," *Commun. ACM*, vol. 24, no. 6, pp. 381–395, Jun. 1981.

[13] K. Kubo, C. Li, S. Ishida *et al.*, "Design of ultra low power vehicle detector utilizing discrete wavelet transform," in *Proc. ITS AP Forum*, May 2018, pp. 1052–1063.

[14] L. Xiaofeng and L. Mingjie, "The de-noising method for EMD threshold based on correlation," in *Proc. IEEE Int. Conf. Signal Processing (ICSP)*, Oct. 2010, pp. 2613–2616.

[15] N. Chatlani and J. J. Soraghan, "EMD-based filtering (EMDF) of low-frequency noise for speech enhancement," *IEEE/ACM Trans. Audio, Speech, Language Process.*, vol. 20, no. 4, pp. 1158–1166, May 2012.

[16] Y. Kopsinis and S. McLaughlin, "Development of EMD-based denoising methods inspired by Wavelet thresholding," *IEEE Trans. Signal Process.*, vol. 57, no. 4, pp. 1351–1362, Apr. 2009.

[17] J. Moragues, L. Vergara, J. Gosálbez *et al.*, "Background noise suppression for acoustic localization by means of an adaptive energy detection approach," in *Proc. IEEE Int. Conf. on Acoustics, Speech, and Signal Processing (ICASSP)*, Mar.–Apr. 2008, pp. 2421–2424.

[18] S. Ganapathi and M. Deivasigamani, "Noise reduction in underwater acoustic signals for tropical and subtropical coastal waters," in *Proc. IEEE/OES China Ocean Acoustics (COA)*, Jan. 2016, pp. 1–6.